ELSEVIER

# CO$_2$-assisted fiber impregnation

Zhihao Shen [a], Gary S. Huvard [b,*], C. Shawn Warriner [b], Mark Mc Hugh [b],
Joseph L. Banyasz [c], Munmaya K. Mishra [c]

[a] *Philip Morris USA Postgraduate Research Program, 4201 Commerce Road, Richmond, VA 23234, USA*
[b] *Department of Chemical and Life Science Engineering, Virginia Commonwealth University, Richmond, VA 23284, USA*
[c] *Philip Morris USA Research Center, 4201 Commerce Road, Richmond, VA 23234, USA*

## Abstract

Near-critical and supercritical CO$_2$ is used to facilitate the impregnation of additives, vanillin and L-menthol, into cellulose acetate (CA). SCF technology applied at low pressures is a viable approach for this application since CO$_2$ only has to dissolve low molecular weight compounds and not the CA fiber. Hence, impregnation operating temperatures are kept under 60 °C and optimum operating pressures are less than 2000 psig and are typically closer to 1250 psig. The optimum operating conditions are intimately linked to the mass transfer and phase behavior characteristics of polymer−CO$_2$, polymer−additive, and additive−CO$_2$ mixtures. It is possible to impregnate up to ∼10 wt% vanillin or L-menthol into CA fiber as verified by gravimetric, TGA, and TGA/MS analyses. SEM analysis of the CA fiber shows that the fiber does not undergo structural changes during this impregnation process even when the fiber is rapidly depressurized. At atmospheric conditions, the additives are in solid form in the CA fiber and slowly diffuse from the fiber at a rate fixed by solid diffusion from a semi-crystalline polymer matrix. Hence, a significant amount of additive is still present in the fiber after one month.
© 2008 Elsevier Ltd. All rights reserved.

## 1. Introduction

For more than 75 years scientists and engineers have been aware that supercritical fluid (SCF) solvents offer the potential of novel processing protocols [1]. However, it is only in the past three decades that SCF solvents have been investigated or applied as solvents for processing foods, nutraceuticals, and polymeric materials, as reaction media for polymerization processes, as environmentally preferable solvents for solution coatings, powder formation, impregnation, encapsulation, cleaning, crystal growth, anti-solvent precipitation, and as mixing/blending aids for crystalline or viscous materials.

Efficient processing schemes can depend intimately on the solute−SCF solvent phase behavior as well as the mass transfer characteristics of the process. For example, it is important to know the solubility of a solute, such as a dye or additive [2−5], in supercritical CO$_2$ to fully assess the potential of using CO$_2$ for impregnation or dyeing processes [6−12].

The impregnation process can be described with the same thermodynamic and mass balance relationships used for the SCF extraction of additives from polymers since these processes are the inverse of one another. It is often not possible to measure the solubility of the additive in neat polymer since additive diffusivity into the polymer is kinetically limited, especially at temperatures well below the polymer glass transition temperature, $T_g$ [13]. However, the effective $T_g$ decreases as CO$_2$, or any other plasticizer, is dissolved into the polymer [14]. The effective $T_g$ can fall below the operating temperature, which means that the polymer−CO$_2$ mixture behaves as a rubber and the additive diffusion rate can increase

by many orders of magnitude compared to the rate into neat glassy polymer. It is important to recognize that although the polymer–$CO_2$ mixture can exhibit the characteristics of a rubber, the presence of $CO_2$ in the polymer can also substantially decrease the solubility of the additive as compared to its solubility in pure polymer. At low $CO_2$ pressures where the polymer still exhibits glassy characteristics, the uptake can be severely limited by an exceedingly low additive diffusivity, $D_{additive}$, even though there exists a large thermodynamic driving force for dissolution of the additive. Conversely, at high $CO_2$ pressures where the polymer swells and exhibits rubbery characteristics, the additive uptake can also be fairly modest due to a lower thermodynamic driving force for additive dissolution, even though the kinetic diffusivity limitation has been reduced. Note that the additive itself can be more effective than $CO_2$ for swelling the polymer and lowering the polymer $T_g$. The difficulty of course is that the equilibrium solubility of the additive cannot be realized at atmospheric operating conditions due to mass transfer limitation. Hence, additive uptake depends in a complex manner on the $CO_2$ pressure, the effective $T_g$ of the polymer relative to the operating temperature, and the thermodynamically controlled solubility of the additive in the pure polymer and in the polymer–$CO_2$ mixture, where the additive itself can significantly swell the polymer and lower the polymer $T_g$.

To demonstrate the interplay of process variables in the impregnation process, illustrative calculations are presented here for the uptake of a hypothetical additive, with a molecular weight of 150, in a hypothetical polymer film $2.54 \times 10^{-3}$ cm thick. Table 1 lists the assumed values for the additive solubility in the polymer and additive diffusivity used for these calculations. The additive is assumed to have a solubility in the polymer relative to the $CO_2$-rich phase (relative solubility) in a range from 10 to 2 (arbitrary) units when the polymer is exposed to $CO_2$ pressures from 500 to 2500 psia, respectively. At a $CO_2$ operating pressure of 500 psia, the hypothetical polymer is assumed to be glassy and $D_{additive}$ is assumed to be $1 \times 10^{-11}$ cm²/s in the polymer–$CO_2$ mixture, which is a reasonable value for an additive with a molecular weight of 150 at these conditions [15]. At a $CO_2$ operating pressure of 1000 psia, the polymer swells and $D_{additive}$ now increases to $2 \times 10^{-10}$ cm²/s, while the additive relative solubility in the new polymer–$CO_2$ mixture drops to 8 units. An increase to a $CO_2$ operating pressure of 1500 psia results in a further five-fold increase in $D_{additive}$ as the polymer–$CO_2$ mixture becomes rubbery at the operating

temperature, however, additive relative solubility now drops to 6 units. A similar progression in the increase in $D$ with increasing $CO_2$ pressure has been demonstrated previously [15] and the typically dramatic increase in $D$ as the glass transition is traversed to the rubbery state has long been established [16,17]. Our calculations also assume the presence of an excess amount of pure additive phase that maintains a saturated additive–$CO_2$ phase during the impregnation process. Although additive diffusion into a glassy polymer–$CO_2$ mixture is apt to be non-Fickian, the computed uptake curves assume Fickian kinetics to capture the dominant, first-order effects of the process variables. Fig. 1 shows that several uptake curves intersect due to the kinetic limitations imposed by the exceedingly low additive diffusivities chosen for the two lower pressures. Ultimately the relative uptakes at 500 and 1000 psia will reach 10 units in 3.5 days and 8 units in 4.5 h, respectively.

Fig. 2 shows the calculated uptake curves in Fig. 1 recast as uptake versus $CO_2$ pressure for a fixed impregnation time. The sharp maximum in the uptake curves in Fig. 2 are a consequence of the balance between the increased additive diffusivity and the reduced thermodynamic driving force for additive solubility in the polymer–$CO_2$ mixture. Note that the uptake declines significantly as the $CO_2$ pressure is increased to high levels and, although not shown here, ultimately the uptake curves superpose at longer experimental contact times.

For the present study, a $CO_2$-assisted batch impregnation process is used to load vanillin or L-menthol into CA fibers without disrupting fiber morphology. The experimental data obtained in the present study are presented in the manner similar to that shown in Fig. 2. Thermogravimetric analysis (TGA) is used to confirm the gravimetrically-measured weight increase of the fibers. In addition, coupled TGA/MS analysis is used to ascertain whether the vanillin or L-menthol is on the outside or inside of the fiber. Scanning electron microscopy (SEM) of the fiber is used to determine whether fiber morphology has changed during processing and also to determine whether the vanillin or L-menthol is on the outside or inside of the fiber.

Table 1
Relative solubilities and diffusivities as a function of pressure for a hypothetical polymer/additive/$CO_2$ impregnation experiment at a fixed temperature

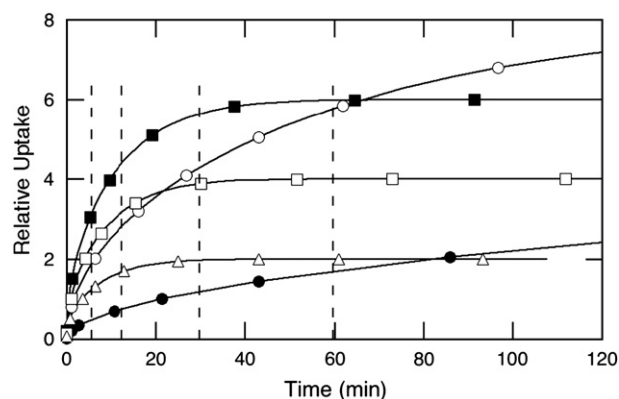| $CO_2$ pressure (psia) | Relative solubility (arbitrary units) | Additive diffusivity (cm²/s) $\times 10^{11}$ |
|---|---|---|
| 500 | 10 | 1 |
| 1000 | 8 | 20 |
| 1500 | 6 | 100 |
| 2000 | 4 | 125 |
| 2500 | 2 | 150 |



Fig. 1. Calculated effect of $CO_2$ pressure on uptake of a hypothetical additive into a thin sheet of polymer. ● – 500 psia, ○ – 1000 psia, ■ – 1500 psia, □ – 2000 psia, △ – 2500 psia. The vertical dashed lines represent the time allotted for an uptake experiment used to generate Fig. 2.
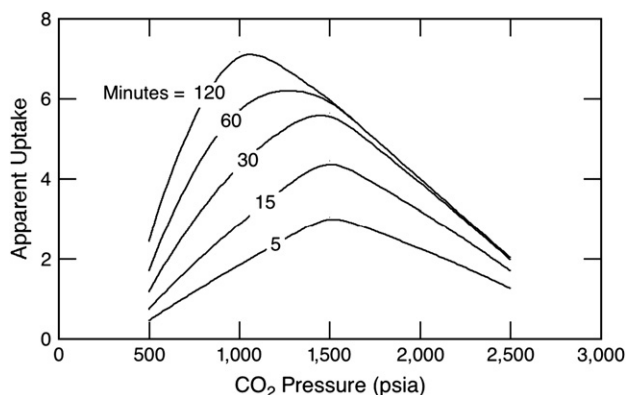
Fig. 2. Effect of time on the apparent isothermal impregnation uptake of an additive in $CO_2$ at different pressures. The different experiment exposure times are noted in the figure.

## 2. Materials

Medical grade $CO_2$ (99.8% minimum purity) was obtained from Roberts Oxygen and used as-received. Vanillin (99%, CAS# 121-33-5, Catalog# V1104) and L-menthol (Kosher, CAS# 2216-51-5, Catalog# W266558) were both obtained from Aldrich and used as-received.

## 3. Experimental technique

Fig. 3 shows a schematic diagram of the high-pressure apparatus (Parr compact lab reactor, Series 5500, 3000 psia maximum operating pressure with a magnetically-coupled stirrer drive) used for the impregnation experiments. A 100 ml vessel was used for the vanillin experiments and a 300 ml vessel was used for the L-menthol experiments. CA fiber, ~1.5 g for the vanillin experiments and ~3.0 g for the L-menthol experiments, was placed in a stainless steel holder to minimize the loss of fibers during the experiment and the holder was attached to the stirrer shaft. The mixing vessel was then loaded with enough solid vanillin or L-menthol, to within ±0.0005 g, to obtain a fiber/additive (g/g) ratio of ~five. A high-pressure bomb was used to transfer 50–100 g (±0.05 g) of $CO_2$ for the vanillin experiments and 140–230 g (±0.05 g) for the L-menthol experiments. The mixing vessel was heated to the desired temperature, constant to within ±1.5 °C, and if the $CO_2$
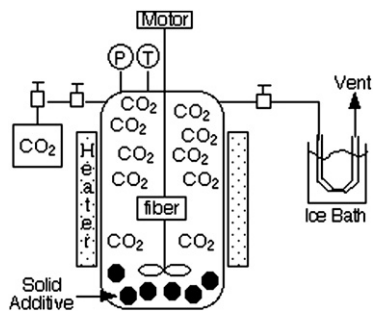


Fig. 3. Schematic diagram of the high-pressure impregnation apparatus used in this study.
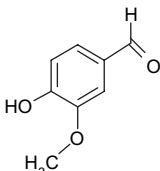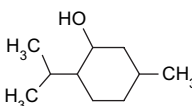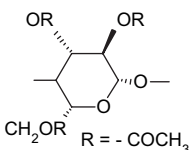
pressure was too high at this point, a small amount of $CO_2$ was vented from the vessel which may result in a small, but inconsequential, amount of additive also being vented from the vessel. Once the pressure was fixed and held constant to within ±40 psia, the vessel was stirred for 30 min to allow the $CO_2$–additive phase to diffuse into the CA fiber. For the majority of the experiments the stirring was then stopped, the mixing vessel was placed in a dry ice–acetone bath, and the $CO_2$ was vented from the vessel. For ~10% of the experiments the $CO_2$ phase was vented from the mixing vessel into a chilled u-tube to trap any additive that dissolved in the $CO_2$. For these experiments the mixing vessel was not first chilled. After decompression, the mixing vessel was dismantled and the fiber was weighed, the additive in the u-tube was weighed, and the amount of any additive remaining in the vessel was also weighed. It was possible to close a mass balance to within 60–95 wt% of the additive loaded in the vessel. The weight loss of the fiber was tracked over several weeks although it should be noted that the fiber was kept in a container open to the environment so that the fiber may have picked up some moisture from the air.

## 4. Results and discussion

Table 2 lists selected properties of vanillin, L-menthol, and cellulose acetate (CA) fiber used in these studies. Both vanillin and L-menthol are polar and contain hydroxyl groups which means that these additives can self- and cross-associate via intramolecular and intermolecular hydrogen bonding. Repeat groups of cellulose acetate may self-associate since the degree of substitution of the CA is ~2.5, which means that the CA repeat groups contains a finite amount of hydroxyl groups. In addition CA is expected to cross-associate with both vanillin and L-menthol. An important variable in the impregnation process is the amount of swelling of the CA fiber, if any, when contacted with high-pressure $CO_2$. Although CA fiber has a very high glass transition temperature ($T_g$) of ~192 °C, it is well known that a substantial reduction in $T_g$ is observed if the polymer absorbs a large amount of a plasticizer, including $CO_2$ [14,18]. Several authors have determined the solubility [19,20] and permeation [19,21] of $CO_2$ in CA. $CO_2$ solubility can reach 12 wt% in CA at 30 °C and a pressure as low as 600 psig [20]. To the best of our knowledge, there are no reports on the magnitude of the $T_g$ depression of CA by $CO_2$ and, using the Chow equation [14], it is easy to show that the calculated depression of $T_g$ by $CO_2$ is no more than ~30 °C, which means that the CA amorphous regions remain glassy at the impregnation operating conditions used in the present study. Stern and De Meringo [20] suggest that $CO_2$ dissolves in the microcavities in CA, which implies that the CA fiber does not have to swell to any great extent to support such a high solubility of $CO_2$. In the present study, the CA fiber did not exhibit a weight increase after soaking in saturated liquid $CO_2$ at ambient temperature for up to 16 h, nor did the rapid depressurization of the $CO_2$ at the end of the soaking experiment have any effect on the fiber structure, as determined by SEM. We suspect that a large fraction of the

Table 2
Structure and physical properties of vanillin, L-menthol, and a cellulose acetate repeat group. The glass transition temperature ($T_g$) of cellulose acetate fiber was measured in our laboratory by DSC. The melting and boiling points of vanillin and L-menthol are reported by Aldrich Co

| Name | Structure | $M_w$ | $T_{melt}$ (°C) | $T_{boil}$ (°C) |
|---|---|---|---|---|
| Vanillin | | 152.2 | 81–83 | 285 |
| L-Menthol | | 156.3 | 45.0 | 212 |
| Cellulose acetate repeat group ~2.5 substitution | | | $T_g = 192$ | |

$CO_2$ is filling the microvoidal regions in the polymer with some of the $CO_2$ dissolving in the amorphous regions of the polymer, which is similar to the conclusions of Stern and De Meringo [20]. However, the dissolution of $CO_2$ in CA is limited since cellulose acetate repeat groups hydrogen bond to one another and $CO_2$ does not have the solvent strength to overcome these CA–CA interactions nor does $CO_2$ participate in hydrogen bonding with hydroxyl groups.

Although both vanillin and L-menthol are solids at room temperature it is important to know the conditions that these two compounds melt in the presence of high-pressure $CO_2$ since the possibility exists that liquid vanillin or L-menthol can be splashed onto the fiber rather than impregnated into the fiber. There is a fair amount of solubility and phase behavior data available in the literature for vanillin [22–27] and a limited amount of data for L-menthol [28,29]. The $CO_2$-assisted impregnation process reported here is operated at temperatures from ambient conditions to 50 °C and pressures to 2500 psia. The phase behavior for the vanillin–$CO_2$ system shown in Fig. 4A indicates that solid vanillin exists at temperatures between ~32 and 65 °C and pressures below 3000 psia, which bracket the operating conditions for the impregnation process. The solid vanillin solubility isotherms at 40 and 60 °C in Fig. 4B indicate that vanillin does not dissolve to a great extent in $CO_2$. Fig. 5 shows that menthol is 10 times more soluble in $CO_2$ than is vanillin at the same temperatures and pressures. Note that menthol liquifies in the presence of $CO_2$ at 35 °C and pressures near ~600 psia. Hence, care must be taken when performing an impregnation experiment with menthol to avoid overloading the mixing vessel which would cause excess liquid menthol to splash onto the fibers.

Vanillin impregnation experiments are performed at 20 and 50 °C and pressures from 820 to 2550 psia. Fig. 6 shows that the increase in CA fiber weight is ~12 wt% when impregnated with vanillin in $CO_2$ at 50 °C. Each data point of both

isotherms shown in Fig. 6 represents conditions used for an independent experiment where the fiber weight is measured at least twice weekly. The data in the figure are 30-day averages since the fiber weight remained virtually constant over this
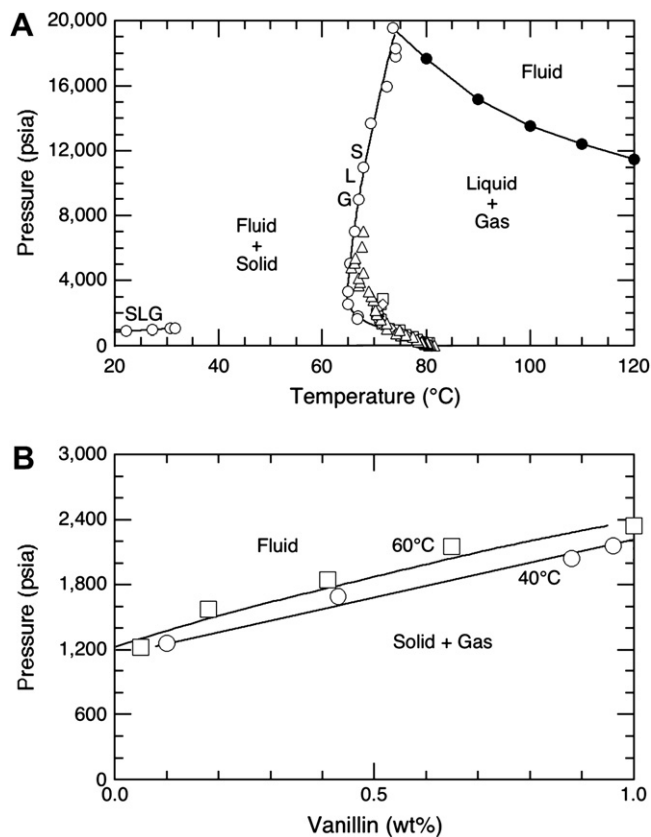


Fig. 4. Phase behavior data for vanillin in $CO_2$: (A) pressure–temperature diagram: S – solid, L – liquid, G – gas. Open circles [23], open squares [21], open diamonds [22], open triangles [25]; (B) solid solubility data [25].
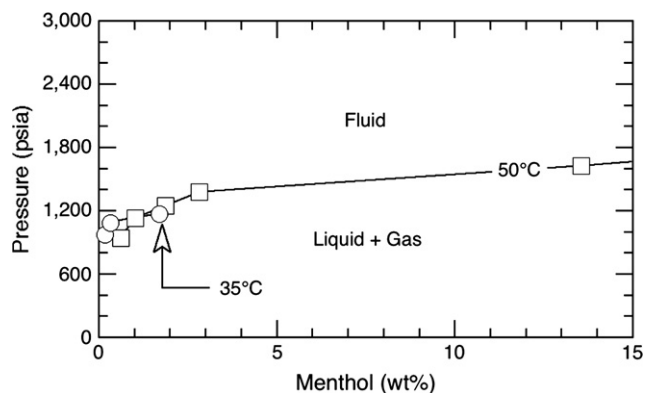
Fig. 5. Solubility of menthol in $CO_2$ [27,28]. Solid circles − 35 °C, open squares − 50 °C.

time period. The error bars on a given data point show the standard deviation of the average weight of the fiber. Immediately after an experiment, the fiber usually exhibits a much higher weight increase although, within ∼1 h, the weight of the fiber stabilizes and remains at the value shown in Fig. 6 for up to one month. It is apparent that near-critical and supercritical $CO_2$ provides a means for impregnating CA fiber with significant amounts of solid vanillin.

Note that the shape of the 50 °C vanillin weight gain curve in Fig. 6 is similar to the shapes of the curves shown in Fig. 2, which suggests that the impregnation process is governed by the mass transfer and thermodynamic considerations previously described in Section 1. The maximum in the observed increase in fiber weight is a consequence of the effect of $CO_2$ present in the polymer-rich phase, which increases the additive diffusivity into the polymer but, at the same time, reduces the thermodynamic driving force for the dissolution of the additive into the polymer. Four experiments were performed at 50 °C and 1500 psia to bracket the influence of contact time on vanillin loading. Duplicate experiments were run at 1 and 2 h with the same 5/1 ratio of fiber/vanillin. A vanillin
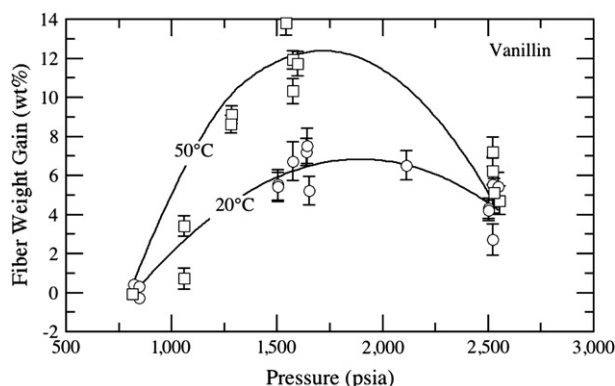
loading of $20 \pm 2$ wt% was obtained for 1 h contact time and $19 \pm 1$ wt% for 2 h contact time. Therefore, the maximum loading must occur at contact times between 30 and 60 min. The increase in the maximum of the 50 °C isotherm at 1500 psia also follows precisely the trends predicted in Fig. 2 where the maximum in the curve would superpose at longer impregnation times. It should be noted that the 50 °C data at 2500 psia were obtained with $CO_2$ unsaturated with vanillin which leads to a slightly lower CA weight gain compared to the gain had $CO_2$ been saturated. Hence, the high-pressure portion of the 50 °C isotherm in Fig. 6 would have exhibited a more gradual reduction in the fiber weight increase than that shown in the figure.

The 20 °C vanillin uptake isotherm in Fig. 6 exhibits similar trends to the 50 °C isotherm, although the CA weight gains at 20 °C are lower than those measured at 50 °C. It should be noted that $CO_2$ at 20 °C is saturated with vanillin regardless of the pressure. There are two, interrelated reasons for the lower uptake of vanillin in CA fiber at 20 °C compared to 50 °C. First, the solubility of vanillin at 20 °C in pure $CO_2$ is expected to be extremely low based on the solubility data at higher temperatures shown in Fig. 4B and the expected solubility of a crystalline solid in $CO_2$ at temperatures lower than the critical temperature of $CO_2$ and the melting point of the solid [1]. Stated differently, solid−solid interactions are much stronger than $CO_2$−solid interactions at these low temperatures which leads to very low solid solubility in $CO_2$. Second, Stern and De Meringo [20] showed that the solubility of $CO_2$ in pure CA is more than a factor of 2 greater at 20 °C than that observed at 50 °C. Hence, the large amount of $CO_2$ that dissolves in the CA fiber serves as an antisolvent that causes the vanillin to precipitate from the CA fiber.

The key result shown in Fig. 6 is that CA fiber can be loaded with solid vanillin far in excess of that possible by other techniques. Also, the data in Fig. 6 show that lower operating pressures are preferred for this $CO_2$-assisted impregnation process, which is a consequence of the balance between mass transfer and thermodynamic considerations that are influenced by the presence of $CO_2$ in the polymer-rich phase. It is also important to note that the physical structure of the vanillin-loaded CA fiber shown in Fig. 7A is identical to that of virgin fiber (not shown here), which suggests that high-pressure $CO_2$ has little effect on the morphology of the fiber. Although not shown here, DSC measurements confirm that there is very little change in the $T_g$ of the CA fiber after loading with vanillin also suggesting that the morphology of the fiber has not undergone any significant change due to this impregnation process.

$CO_2$-assisted impregnation experiments are performed with L-menthol at 30 and 40 °C and pressures of 750–2520 psia. The L-menthol fiber impregnation data in Fig. 8 exhibit similar trends to those of vanillin, although now the maximum in loading with pressure is much sharper than the maxima with vanillin shown in Fig. 6. The optimum operating conditions with menthol were 40 °C and 1000 psia, which results in a menthol loading of ∼6 wt% compared to ∼14 wt% for vanillin. These experiments were operated with 0.3–0.4 wt%
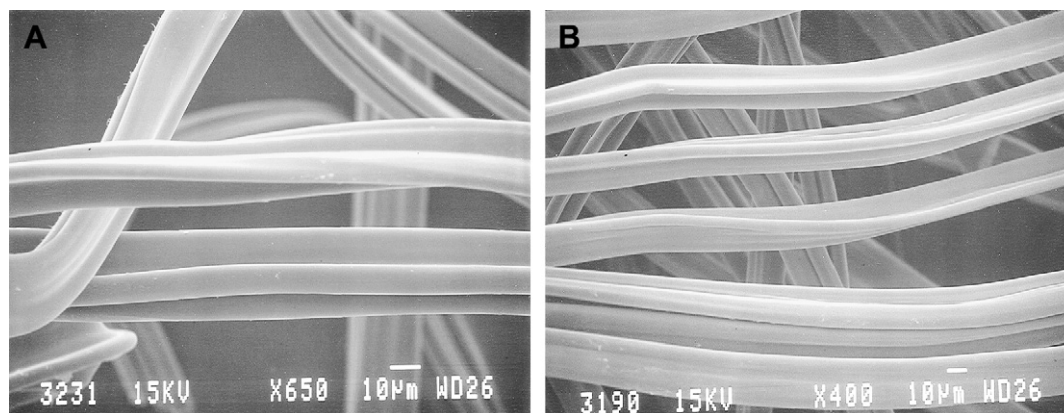


Fig. 6. Weight gain of CA fiber after $CO_2$-assisted impregnation of vanillin at 20 °C (open circles) and 50 °C (open squares) and pressures from 750 to 2500 psia. The data represent the average weight increase of the fiber obtained at least twice weekly over a 30-day period after the impregnation experiment. The error bars represent the standard deviation of the average weight increase. The lines are drawn to guide the eye.

Fig. 7. Typical SEM pictures of CA fiber impregnated with (A) 14.9 wt% vanillin (processed in $CO_2$ at 40 °C and 1300 psia) and (B) 3.6 wt% L-menthol (processed in $CO_2$ at 30 °C and 1050 psia).

menthol in the $CO_2$-rich phase. However, the phase behavior in Figs. 4 and 5 indicate that L-menthol is 10 times more soluble than vanillin in $CO_2$. Hence, the $CO_2$-rich carrier phase is much further from saturation with menthol as compared to vanillin, which means that the partitioning of menthol favors the $CO_2$-rich phase rather than the CA fiber. Several menthol experiments were performed with a fiber/additive ratio of 2 and 0.25 so that increased amounts of menthol were charged to the vessel. Unfortunately the fibers from these experiments were coated with significant amounts of menthol which likely occurs when menthol, liquified in the presence of $CO_2$, is splashed onto the fiber holder during stirring. These anomalous data are ignored in this study. As with the vanillin-loaded fibers, the physical structure of the L-menthol-loaded CA fibers shown in Fig. 7B suggests that there are no structural changes in the fiber due to the menthol or $CO_2$. Although not shown here, DSC measurements again confirm that there is very little change in the $T_g$ of the CA fiber after loading with L-menthol also suggesting that the morphology of the fiber has not

undergone any significant change due to this impregnation process. A dynamic flow apparatus is needed to efficiently impregnate fiber loading with a solute that is highly soluble in $CO_2$, such as L-menthol.

TGA analysis is used to confirm the gravimetrically-measured weight increase of the fibers. In addition, the TGA analysis is also used to ascertain whether the vanillin or L-menthol coats the outside of the fiber or is located inside of the fiber. The CA fiber used in this study has a glass transition temperature at ∼195 °C and the melting points of vanillin and L-menthol are 82 and 45 °C, respectively. Fig. 9 shows a comparison of TGA runs for several different fiber configurations. TGA results are compared for $CO_2$−vanillin-treated CA fiber, virgin CA fiber physically mixed with solid vanillin, CA fiber sprayed with a vanillin−ethanol solution that has vanillin primarily on the outside of the fiber, and pure solid vanillin. The sample sizes for the TGA runs were all approximately the same and the concentration of vanillin in or on the fibers are all close to one another. The $CO_2$−vanillin-treated CA fiber
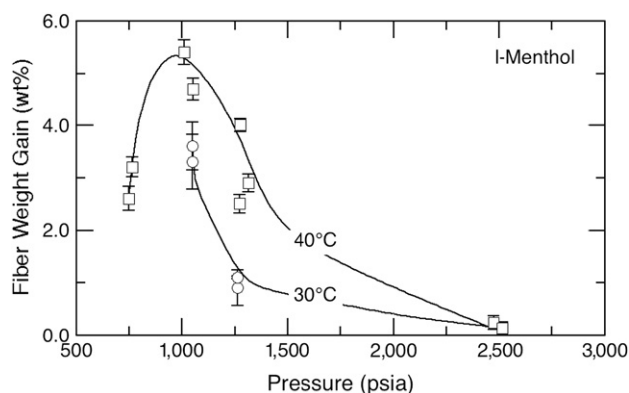


Fig. 8. Weight gain of CA fiber after $CO_2$-assisted impregnation of L-menthol at 30 °C (open circles) and 40 °C (open squares) and pressures from approximately 750−2500 psia. The data in this figure are the average weight increase of the fiber over a 23 day period after the impregnation experiment and the error bars shown in the figure represent the standard deviation of the average weight increase that is measured at least twice weekly over the entire time period. The lines are drawn to guide the eyes. Note that there are two 30 °C data points at ∼2500 psia that are hidden by the 40 °C data at this pressure.
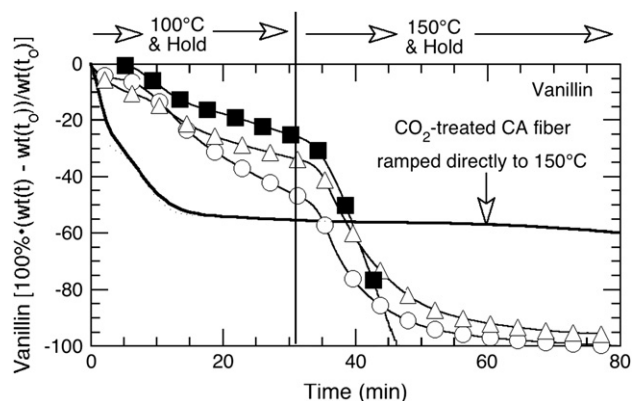


Fig. 9. Comparison of the vanillin weight loss for several different fiber configurations with approximately the same vanillin loading (solvent-free basis). Open circles − 13.6 wt% solid vanillin physically wrapped with CA fibers; open triangles − 13.5 wt% vanillin (solvent-free basis) dissolved in ethanol and sprayed onto CA fiber; solid squares − pure solid vanillin; line − CA fiber impregnated with 9.1 wt% vanillin using $CO_2$ at 50 °C and 1290 psia. Note that the $CO_2$-treated CA fiber was ramped directly to 150 °C and held at that temperature rather than first ramping to 100 °C.

loses ∼60 wt% of the available vanillin within 10 min, but then these fibers only very slowly release a few weight percent of the remaining 40 wt% vanillin over 60 min even though the temperature is increased to 150 °C. In contrast, the vanillin-sprayed fiber and the CA fiber physically mixed with solid vanillin rapidly lose ∼30 wt% of available vanillin within the first 30 min of the TGA run where the temperature is quickly ramped to 100 °C. The remaining vanillin is released from these two fiber samples within 10 min after the temperature is ramped to 150 °C. It is interesting that the weight loss curve for pure solid vanillin closely mimics those for the sprayed fiber and fiber plus vanillin solid mixture. These TGA results suggest that vanillin resides inside the $CO_2$-treated fiber rather than on the outer surface of the fiber.

Fig. 10 is a post-TGA SEM picture of CA fiber originally impregnated with 14.9 wt% vanillin using $CO_2$ at 40 °C and 1265 psia. For this TGA run the furnace temperature was quickly ramped to 150 °C, held at this temperature for 10 min, and then ramped to 220 °C and held for 30 min. Fig. 7A shows the companion SEM picture for the pre-TGA fiber. After the TGA run deposits are visible on the skin of the CA fiber which likely are vanillin that has diffused to the surface but has not yet evaporated from the surface. The TGA data strongly suggest that $CO_2$−vanillin-treated fiber has vanillin incorporated in, rather than on, the fiber. Similar SEM pictures and TGA traces are observed for the $CO_2$−menthol treated CA fiber with the exception that the release events observed with the TGA analysis occur at lower operating temperatures since L-menthol melts at a much lower temperature.

TGA/MS is used to relate the decrease in fiber weight upon heating to the release of vanillin or menthol. Fig. 11 shows the CA fiber weight loss and the simultaneous menthol signals from TGA/MS analysis for a CA fiber impregnated with 2.5 wt% menthol using $CO_2$ at 40 °C and 1250 psia. The first set of peaks in the MS trace that begin at ∼180 °C, peak at ∼200 °C, which is just above $T_g$ for CA fiber, and return to
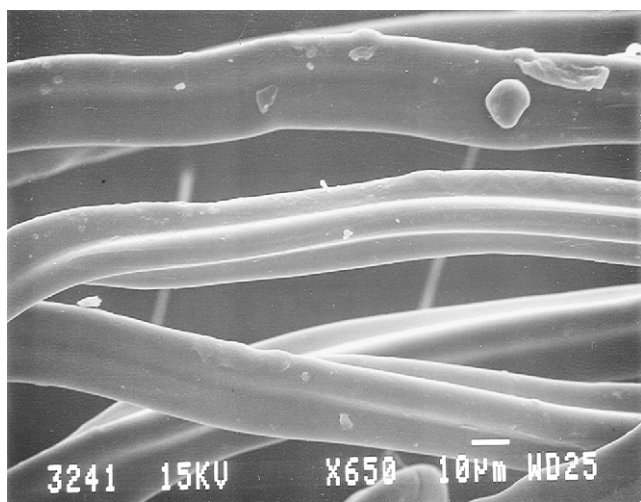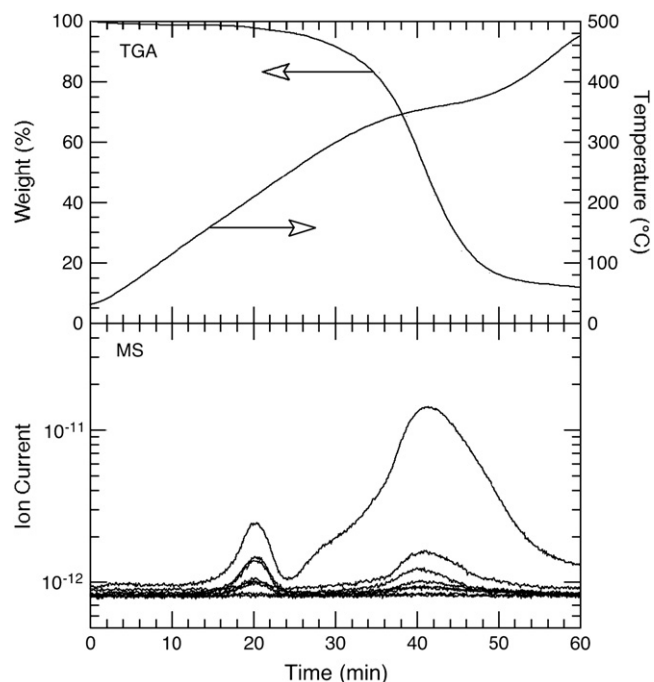


Fig. 11. TGA/MS scan of CA fiber originally impregnated with 2.5 wt% L-menthol using $CO_2$ at 40 °C and 1250 psia.

the baseline at ∼240 °C, correspond to the release of menthol embedded in the CA fiber. The multiple MS peaks at 20 min result from menthol degradation products. The next set of peaks at 42 min in the MS trace correspond to a temperature of ∼360 °C and the weight loss at these high temperatures is associated with the degradation of CA fiber [30,31], resulting in the release of menthol embedded deeper inside the CA fibers. Very similar TGA/MS results are obtained for CA fibers loaded with 3 to 6 wt% menthol.

## 5. Conclusions

It is possible to load CA fiber with different additives using $CO_2$ at modest temperatures and pressures. $CO_2$ is an effective carrier fluid that greatly enhances the impregnation level of high molecular weight additives. Additive uptake by the fiber depends in a complex manner on the $CO_2$ pressure, the effective $T_g$ of the polymer relative to the operating temperature, and the thermodynamically controlled solubility of the additive in the pure polymer and in the polymer−$CO_2$ mixture, where the additive itself can significantly swell the polymer and lower the polymer $T_g$. Nevertheless, the impregnation process can be adequately described with the same thermodynamic and mass balance relationships used for the SCF extraction of additives from polymers since these processes are the inverse of one another. It is interesting that, for this process, the impregnation process is more effective when operated at low rather than high pressure. We are currently extending this impregnation process to additives that are insoluble in $CO_2$ by first dissolving the additive in a liquid solvent that easily dissolves in $CO_2$ but does not readily dissolve the CA fiber. For example, in preliminary experiments we have



Fig. 10. Post-TGA SEM pictures of CA fiber impregnated with 14.9 wt% vanillin using $CO_2$ at 40 °C and 1300 psia. The TGA was ramped to 150 °C, held at this temperature for 10 min, and then ramped to 220 °C and held for 30 min. The companion, pre-TGA SEM picture is shown in Fig. 7A.

been able to impregnate 12–13.5 wt% vanillin in CA fiber at 40 °C and 1275 psia by first dissolving the vanillin in ethanol (33 wt% vanillin). The ethanol–vanillin solution dissolves completely in $CO_2$ at process conditions, the vanillin partitions to the fiber, and the ethanol is flushed from the vessel at the end of the process leaving dry CA fiber with virtually no ethanol.

## Acknowledgments

## References

[1] Mc Hugh MA, Krukonis VJ. Supercritical fluid extraction, principles and practice. 2nd ed. Boston, MA: Butterworth-Heinemann; 1994.

[2] Joung SN, Yoo K-P. Journal of Chemical and Engineering Data 1998;43:9–12.

[3] Kautz CB, Wagner B, Schneider GM. Journal of Supercritical Fluids 1998;13:43–7.

[4] Ozcan AS, Clifford AA, Bartle KD, Lewis DM. Journal of Chemical and Engineering Data 1997;42:590–2.

[5] Tuma D, Schneider GM. Journal of Supercritical Fluids 1998;13:37.

[6] Knittel D, Saus W, Hoger S, Schollmeyer E. Angewandte Makromolekulare Chemie 2003;218:69–79.

[7] Knittel D, Saus W, Schollmeyer E. Journal of Fibre and Textile Research 1997;22:184–9.

[8] Liao SK. Journal of Polymer Research 2004;11:285–91.

[9] Muth O, Hirth T, Vogel H. Journal of Supercritical Fluids 2000;17:65–72.

[10] Santos WLF, Porto MF, Muniz EC, Povh NP, Rubira AF. Journal of Supercritical Fluids 2001;19:177–85.

[11] Watkins JJ, McCarthy TJ. Macromolecules 1994;27:4845–7.

[12] Watkins JJ, McCarthy TJ. Macromolecules 1995;28:4067–74.

[13] Berens AR, Huvard GS. Supercritical fluid science and technology, vol. 404; 1989 [chapter 14].

[14] Chow TS. Macromolecules 1980;13:362–4.

[15] Berens AR, Huvard GS, Korsmeyer RW, Kunig FW. Journal of Applied Polymer Science 1992;46:231–42.

[16] Crank J, Park GS. Diffusion in polymers. London: Academic Press; 1968. p. 96.

[17] Kishimoto A. Journal of Polymer Science, Part A: General Papers 1964;2:1421–39.

[18] Hachisuka H, Sato T, Tohru I, Tsujita Y, Takizawa A, Kinoshita T. Polymer Journal 1990;22:77–9.

[19] Sada E, Kumazawa H, Yoshio Y, Wang S-T, Xu P. Journal of Polymer Science, Part B: Polymer Physics 1998;26:1035–48.

[20] Stern SA, De Meringo AH. Journal of Polymer Science: Polymer Physics Edition 1978;16:735–51.

[21] Houde AY, Krishnakumar B, Charati SG, Stern SA. Journal of Applied Polymer Science 1996;62:2181–92.

[22] Funke-Kokot K, Konig A, Knez Z, Skerget M. Fluid Phase Equilibria 2000;173:297–310.

[23] Funke-Kokot K, Skerget M, Konig A, Knez Z. Fluid Phase Equilibria 2003;205:233–47.

[24] Liu J, Kim YC, Mc Hugh MA. Journal of Supercritical Fluids, 2006;39:201–5.

[25] Selli E, Pome N, Beltrame PL, Mossa A, Testa G, Seves A. Angewandte Makromolekulare Chemie 1999;270:76–80.

[26] Skerget M, Cretnik L, Knez Z, Skrinjar M. Fluid Phase Equilibria 2005;231:11–9.

[27] Wells PA, Chaplin RP, Foster NR. Journal of Supercritical Fluids 1990;3:8–14.

[28] Mukhopadhyay M, De SK. Journal of Chemical and Engineering Data 1995;40:909–13.

[29] Sovova H, Jez J. Journal of Chemical and Engineering Data 1994;39:840–1.

[30] Jain RK, Lal K, Bhatnagar HL. Polymer Degradation and Stability 1989;26:101–12.

[31] Lucena MdCC, de Alencar AEV, Mazzeto SE, Soares SdA. Polymer Degradation and Stability 2003;80:149–55.